A new approach for broad-band omnidirectional antireflection coatings

S. Dutta Gupta[1] **and G. S. Agarwal**[2]

[1]*School of Physics, University of Hyderabad, Hyderabad 500046, India*
[2]*Department of Physics, Oklahoma State University, Stillwater, OK 74078, USA*
sdgsp@uohyd.ernet.in

Abstract: It is shown that broad-band antireflection coatings with extra large angular range can be designed based on the concept of reflectionless potentials. Numerical calculations for inhomogeneous films with or without substrate demonstrate the above capabilities for both TE and TM polarizations. The design possibilities are infinite and the underlying concept does not rely on standard use of quarter wave plates. Suitable inhomogeneous layers on both sides of a lossless thin dielectric film can thus render it invisible.

OCIS codes: (310.1620) Coatings; (310.1210) Antireflection.

References and links

1. H. Sankur and W. H. Southwell, "Broadband gradient-index antireflection coating for ZnSe," Appl. Opt. **23**, 2770-2773 (1984).
2. D. Poitras and J. A. Dobrowolski, "Toward perfect antireflection coatings. 2. Theory," Appl. Opt. **43**, 1286-1294 (2004).
3. Philippe Lalanne and G Michael Morris, "Antireflection behavior of silicon subwavelength periodic structures for visible light," Nanotechnology **8**, 53-56 (1997).
4. Q. Tanga, S. Ogura, M. Yamasaki and K. Kikuchi, "Experimental study on intermediate and gradient index dielectric thin films by a novel reactive sputtering method," J. Vac. Sci. Technol. A **15**, 2670-2672 (1997).
5. K. Kintaka, J. Nishii, A. Mizutani, H. Kikuta and H. Nakano, "Antireflection microstructures fabricated upon fluorine-doped SiO_2 films," Opt. Lett. **26**, 1642-1644 (2001).
6. I. Kay and H. E. Moses, "Reflectionless transmission through dielectrics and scattering potentials," J. Appl. Phys. **27**, 1503-1508 (1956).
7. H. B. Thacker, C. Quigg and J. L. Rosner, "Inverse scattering problem for quarkonium systems. I. One-dimensional formalism and methodology," Phys. Rev. D **18**, 274-286 (1978).
8. J. F. Schonfeld, W. Kwong, J. L. Rosner, C. Quigg and H. B. Thacker, "On the convergence of reflectionless approximation to confining potentials," Ann. Phys.**12**, 1-28 (1980).
9. P. G. Drazin, et al, *Solitons- An Introduction*, 2nd edition (Cambridge University Press, Cambridge, 1989) Ch.3.
10. J. B. Pendry, D. Schurig and D. R. Smith, "Controlling electromagnetic fields," Science **312**, 1780-1782 (2006).
11. U. Leonhardt, "Optical conformal mapping," Science **312**, 1777-1780 (2006).
12. F. J. Garcia de Abajo, G. Gomez-Santos, L. A. Blanco, A. G. Borisov, and S. V. Shabanov, "Tunneling mechanisms of light transmission through metallic films", Phys. Rev. Lett. **95**, 067403 (2005).
13. J. W. Lee, M. A. Seo, J. Y. Sohn, Y. H. Ahn and D. S. Kim, "Invisible plasmonic meta-materials through impedance matching to vacuum," Opt. Express **13**, 10681-10687 (2005).
14. G. W. Milton and N. A. Nicorovici, "On the cloaking effects associated with anomalous localised resonance", Proceedings London Royal Society A **462**, 3027-3059 (2006).
15. F. Zolla, S. Guenneau, A. Nicolet and J. B. Pendry, "Electromagnetic analysis of cylindrical invisibility cloaks and the mirage effect," Opt. Lett. **32**, 1069-1071 (2007).
16. N. Kiriushcheva and S. Kuzmin, "Scattering of a Gaussian wave packet by a reflectionless potential," Am. J. Phys. **66**, 867-872 (1988).
17. S. Zaitsu, T. Jitsuno, M. Nakatsuka and T. Yamanaka, "Optical thin films consisting of nanoscale laminated layers," Appl. Phys. Lett. **80**, 2442-2444 (2002).
18. A. Kasikov, J. Aarik, H. Mandar, M. Moppel, M. Pars and T. Uustare, "Refractive index gradients in TiO_2 thin films grown by atomic layer deposition," J. Phys. D: Appl. Phys. **39**, 54-60 (2006).

#82452 - $15.00 USD Received 26 Apr 2007; revised 3 Jul 2007; accepted 5 Jul 2007; published 18 Jul 2007

1. Introduction

It is now well understood that any inhomogeneity in an otherwise homogeneous medium can cause reflection. For example, an interface between two dielectrics results in a reflected light for waves incident on the interface from any of the media. The measure of reflection is the intensity reflection coefficient which is the ratio of the intensity of the reflected light to that of the incident light. For nonmagnetic media, it depends on the polarization of the incident light, the angle of incidence, the dielectric constants of the media and also the wavelength of light, since the optical properties may depend on the wavelength (referred to as dispersion). It is often a must for optical instrumentation to suppress reflection at the many interfaces of the optical components in order to increase the light throughput. Usually this is achieved by $\lambda/4$ antireflection coatings with refractive index intermediate between those of the medium of incidence and the substrate. The physical principle that enables the operation of a $\lambda/4$ plate is the fact that waves reflected back in the medium of incidence from the two interfaces cancel each other in a destructive interference. Clearly for a given polarization and for given angle of incidence, this can be achieved only at a given wavelength. Thus disturbing any parameter like wavelength or the angle of incidence or the polarization can offset the destructive interference leading to finite reflection. Though there have been many schemes with multiple layers or with variable refractive index profiles, most of the antireflection coatings today[3, 4, 5] suffer from limited bandwidths as well as very restricted range of angles of incidence for satisfactory operation. The films designed for a particular wavelength range and angle are not suitable for other purposes, thus, eliminating the off-the-shelf, immediate delivery of such components.

In this paper, we suggest a scheme of designing one dimensional refractive index profiles which does not rely on quarter wave plates. The scheme is based on the *rigorous and exact* theoretical foundation of reflectionless potentials which were proposed by Kay and Moses [6] and later studied in great detail in the context of inverse scattering theory [7, 8, 9]. To the best of our knowledge the concept of reflectionless potentials has never been used to design antireflection coatings. Note also that other schemes of variable profiles like linear or quintics[1] or their variations[2] do not have rigorous theoretical justification. We show that realistic index profiles based on the reflectionless potentials can lead to almost-omnidirectional antireflection coatings with extremely large ranges of wavelength for both TE and TM polarizations. In fact, the choice of such profiles is truly infinite. We record at the outset that we have to generalize the work of Kay and Moses in several important directions to account for practical considerations. Kay and Moses deal with potentials that extend from $-\infty$ to ∞, however any practical coating has to be like several micron thick. Moreover the coating would usually be on a substrate whose presence is to be accounted for. Further the propagation of TM waves is described by a differential Eq. that is not equivalent to Schrodinger Eq.

It is interesting to note that by deposition of suitable refractive index profiles on the two sides of any lossless thin film, the same can be rendered invisible. We emphasize that this invisibility is for a large range of angles and also over a broad frequency span. Thus it is quite different from the recent proposal of Pendry [10] and Leonhardt [11] as well as other related work [12, 13, 14, 15] for achieving invisibility.

In what follows, we present a detailed step-by-step procedure of how to construct such refractive index profiles with or without a substrate, which may lead to total transmission. Since any realistic system is bound to be finite, we truncate the refractive index profile and calculate the reflection coefficient for both TE and TM polarizations. As mentioned earlier, the possibilities are infinite. We pick one representative example and show the feasibility of having extremely low reflection over very broad ranges of frequencies and angles.

#82452 - $15.00 USD Received 26 Apr 2007; revised 3 Jul 2007; accepted 5 Jul 2007; published 18 Jul 2007

2. Propagation equations for TE and TM polarized waves and the reflectionless index profiles

Consider a nonmagnetic ($\mu = 1$) stratified medium with the dielectric function varying as $\varepsilon = \varepsilon(z)$. Initially we consider the case when $\varepsilon(z) = \varepsilon_s$ as $z \to \pm\infty$, though this will be relaxed later to incorporate the effect of a substrate. Any incident plane wave with arbitrary polarization can be considered to be a mixture of two independent polarizations, namely, the TE (transverse electric) or the TM (transverse magnetic). The TE (TM) wave has only one non-vanishing electric (magnetic) field component perpendicular to the plane of incidence (say, xz plane). Assuming a temporal dependance $e^{-i\omega t}$, the propagation Eqs. for the electric field $\vec{\mathbf{E}} = (0, \mathscr{E}e^{ik_x x}, 0)$ of the TE waves and the magnetic field $\vec{\mathbf{H}} = (0, \mathscr{H}e^{ik_x x}, 0)$ of TM waves can be written as

$$\frac{d^2\mathscr{E}}{dz^2} + (k_0^2\varepsilon(z) - k_x^2)\mathscr{E} = 0, \tag{1}$$

$$\frac{d^2\mathscr{H}}{dz^2} - \frac{d\mathscr{H}}{dz}\frac{d(\ln\varepsilon(z))}{dz} + (k_0^2\varepsilon(z) - k_x^2)\mathscr{H} = 0, \tag{2}$$

where $k_x = k_0\sqrt{\varepsilon_s}\sin\theta$ is the x-component of the vector for wave incident at $-\infty$ at an angle θ and $k_0 = \frac{\omega}{c}$ is the free space wave vector. For a given $\varepsilon(z)$ profile introducing E and $V(z)$ as

$$V(z) = k_0^2\varepsilon_s - k_0^2\varepsilon(z). \tag{3}$$

$$E = k_0^2\varepsilon_s\cos^2\theta. \tag{4}$$

Eq.(1) can be recast in the form of stationary Schrödinger Eq. with energy E and potential $V(z)$

$$\frac{d^2\psi}{dz^2} + (E - V(z))\psi = 0. \tag{5}$$

The potential $V(z)$ in Eq.(5) is said to be reflectionless[6] if any wave with arbitrary positive energy can pass through the potential completely. It is also clear that Eq.(3) establishes the relation between the reflectionless potential and the corresponding dielectric function profile $\varepsilon(z)$. Since refractive index is given by the square root of the dielectric function, Eq.(3) can be rewritten to yield the corresponding relectionless refractive index profile $n(z)$ as

$$n^2(z) = n_s^2 - \frac{V(z)}{k_0^2} \;\; ; \;\; \varepsilon_s = n_s^2. \tag{6}$$

Due to the presence of the log derivative of the profile $\varepsilon(z)$ in (2), similar feat leading to an Eq. like (6) is not achievable for the TM-waves. Eq.(4) clearly indicates that a change in the angle corresponds to a change in the energy (albeit in a finite domain) in the corresponding quantum problem. It is thus possible to talk about reflectionless dielectric function profiles for all possible angles of incidence for a given wavelength. As will be shown later such omnidirectional 'total' transmission exists even for realistic *i.e.* truncated (finite domain) $\varepsilon(z)$ profiles. However, designing a profile that is reflectionless for both TE and TM waves is not possible (compare Eqs.(1) and (2)). Fortunately, as we will see reflectionless profiles for TE waves turns out to be almost reflectionless even for TM -waves for large angular domains. The situation is a bit more involved in case of wavelength dependence. As is clear from Eq.(6) that the index profile $n(z)$ depends on the wavelength. Potential designed to be reflectionless at one wavelength is not reflectionless at other wavelengths. Fortunately again, the deviation from total transmission at lower wavelengths is not significant. We thus found that the dielectric function profiles based on

#82452 - $15.00 USD Received 26 Apr 2007; revised 3 Jul 2007; accepted 5 Jul 2007; published 18 Jul 2007

reflectionless potentials can offer flat response almost with total transmission over large angle and wavelength regions.

In what follows, we briefly outline the scheme to construct the reflectionless potentials [6] and the corresponding refractive index profiles (see Eq.(6)). Several theorems developed by Kay and Moses[6], prove to be handy in achieving the goal. Without going into the statements of the theorem, we present the relevant steps. Assume that $2N$ positive arbitrary constants $A_1, A_2, \cdots A_N$ and $\kappa_1, \kappa_2, \cdots \kappa_N$, are *given*. One then carries out the following steps

1. One considers the following set of simultaneous linear Eqs.

$$\sum_{j=1}^{N} M_{ij} f_j(z) = -A_i e^{\kappa_i z}, M_{ij} = \delta_{ij} + \frac{A_i e^{(\kappa_i+\kappa_j)z}}{(\kappa_i+\kappa_j)}. \tag{7}$$

   In Eq.(7) $-\kappa_n^2$ and $f_n(z)$ have the physical meaning of the eigenvalue and eigenfunction of the corresponding Sturm-Liouville problem with $V(z)$ in Eq.(5) representing the reflectionless potential and the matrix M has a non vanishing positive determinant [6].

2. Construct the determinant $D = |M_{ij}|$ of the coefficient matrix in Eq.(7).

3. Then the reflectionless potential $V(z)$ is given by

$$V(z) = -2\frac{d^2}{dz^2}[\log(D)]. \tag{8}$$

4. As per Eq.(6) the corresponding index profile $n(z)$ is given by

$$n^2(z) = n_s^2 + \frac{2}{k_0^2}\frac{d^2}{dz^2}[\log(D)]. \tag{9}$$

Note that D is determined from M_{ij} which in turn are determined by the choice of the free parameters A_i, κ_i. We give some examples–If we consider only one non-vanishing A_1 and κ_1 with $A_1 = 2\kappa_1$ then we get

$$D(z) = 1 + e^{2\kappa_1 z} \;\; ; \;\; n^2(z) = n_s^2 + \frac{2\kappa_1^2}{k_0^2} Sech^2(\kappa_1 z) \tag{10}$$

With the choice $A_1 = 2\kappa_1$, we chose the maximum of (10) *i.e.*the refractive index at $z = 0$. The potential corresponding to the *sech* profile in Eq.(10) is usually referred to as Poschl-Teller (PT) potential and has been studied in detail [16]. Further for the 2-parameter family $A_1, A_2 \neq 0$, we get

$$D(z) = 1 + \frac{A_1}{2\kappa_1} e^{2\kappa_1 z} + \frac{A_2}{2\kappa_2} e^{2\kappa_2 z} + \frac{(\kappa_1-\kappa_2)^2 A_1 A_2 e^{2(\kappa_1+\kappa_2)z}}{4\kappa_1\kappa_2(\kappa_1+\kappa_2)^2}, \tag{11}$$

Thus increasingly complex refractive index profiles result with increase in the number of parameters. Our simulations, have shown that we achieve satisfactory results over large wavelength range and large angles of incidence by working with four parameter family. Note that since the possibilities are infinite, better performance with lower parameter families is not ruled out. It is pertinent to comment on the choice of constants A's and κ's in (8) and (9). For defining the potential (8), mathematically there are no constraints on them except their reality and non-negativity. However, since the refractive index values are *very much limited for realistic*

#82452 - $15.00 USD Received 26 Apr 2007; revised 3 Jul 2007; accepted 5 Jul 2007; published 18 Jul 2007

materials, one has to exercise great care in choosing the constants, so as not to end up with unphysical values. Besides, any *engineered inhomogeneous system* needs to be *finite* in contrast to the profile (6) (or (9)), which is defined on infinite support. It is thus necessary to look at finite profiles and investigate the deviations from truly reflectionless behavior. Finally the thin AR coatings are to be deposited on a substrate. In order to *implement* the *substrate effects* we consider the profile built on a smooth hyperbolic-tangent ramp

$$n^2(z) = n_{s1}^2 + \frac{2}{k_0^2}\frac{d^2}{dz^2}[\log(D)] + \frac{n_{s2}^2 - n_{s1}^2}{2}[1 + \tanh(\kappa_1 z)], \tag{12}$$

where n_{s1} and n_{s2} are the refractive indices of the bounding media on the left and right of the inhomogeneous medium, respectively.

3. Numerical results and discussions

In this section we present our results on the reflection coefficient from the inhomogeneous film with or without substrate. Initially we use a four parameter family refractive index profile. Later we consider other parameter families to bring out certain salient features. It is clear that for profiles with more than two parameter families one cannot write down compact expressions like (11). One has to resort to numerical simulation. We now present one typical example. As mentioned earlier, one has to exercise great caution in choosing the constants so as not to end up with unphysical values for $n(z)$. Once the design wavelength has been chosen, the practical guideline is offered by the profile (10). For example, for a given λ, using the extremal value of $V(z)$, e.g., $-2\kappa_1^2$ in Eq.(6), one can estimate the value of κ_1 using the following Eq.

$$\kappa_1 = (\pi/\lambda)\sqrt{2(n_{max}^2 - n_s^2)}, \tag{13}$$

where n_{max} is the peak value of the refractive index profile corresponding to (10). For example, for $\lambda = 1.06\mu m$, $n_s = 1.0$, $n_{max} = 1.65$, Eq.(13) yields a rounded value of κ_1 as 5.5 μm^{-1}. Henceforth, assuming the length unit to be micron, we will suppress all the units in the constants. Thus for the simplest reflectionless index profile one has $\kappa_1 = 5.5$ and $A_1 = 2\kappa_1 = 11.0$. We now discuss the effect of additional three pairs of constants of the four parameter family on this profile. If the eigenvalues κ_j's are well separated, then the localized profile remains localized, albeit with some distortions. On the other hand, closely spaced eigenvalues lead to profiles with distinct peaks. The values of A_j's do not affect qualitatively the shape of the profile. Keeping the aforesaid in mind, we choose the parameters as $A_1 = 11, A_2 = A_3 = A_4 = 3.0$, $\kappa_1 = 5.5, \kappa_2 = 0.1, \kappa_3 = 1.0, \kappa_4 = 9.0$.

The resulting refractive index profiles *without or with the substrate* are shown in the insets of Fig. 1. The inhomogeneous film is assumed to occupy a region $-3\mu m \le z \le 3\mu m$ beyond which the left medium is assumed to be air ($n_s = n_{s1} = 1.0$), while the substrate is assumed to have a refractive index 1.4 ($n_{s2} = 1.4$). We also used the same set of constants but at a different wavelength ($\lambda = 1.55\mu m$) leading to an analogous profile with a larger peak value of refractive index (see inset of Fig. 2). For numerical simulations we use a *transfer matrix technique* invoking a fine subdivision and a step-wise constant approximation of the smooth profile. We calculate both the angle and the wavelength dependence of the reflection coefficient. The angle (of incidence) dependence of the intensity reflection coefficient R at $\lambda = 1.06\mu m$ ($\lambda = 1.55\mu m$) for the film in absence or presence of the substrate is shown in Figs. **??**(a) (2(a)) and **??**(b) (**??**(b)), respectively. The solid (dashed) curves in these Figs. are for the TE (TM) polarization. One can easily note the flat response over a very large angular range for both the polarizations. The substrate, while retaining this feature, evens out the differences in response for the two

#82452 - $15.00 USD Received 26 Apr 2007; revised 3 Jul 2007; accepted 5 Jul 2007; published 18 Jul 2007

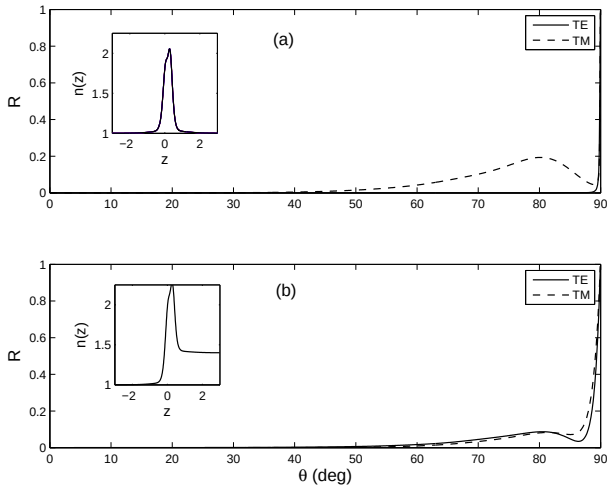

Fig. 1. Intensity reflection coefficient R as a function of angle of incidence θ for the inhomogeneous film (see text for a description) (a) without or (b) with the substrate at $\lambda = 1.06\mu m$. The insets show the refractive index profiles.

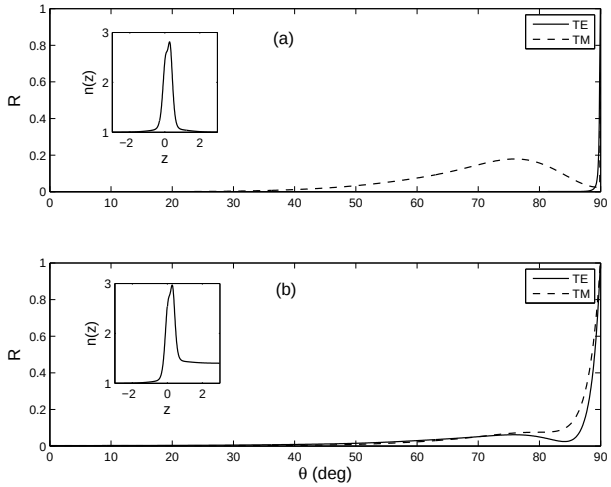

Fig. 2. Intensity reflection coefficient R as a function of angle of incidence θ for the inhomogeneous film (see text for a description) (a) without or (b) with the substrate at $\lambda = 1.55\mu m$. The insets show the refractive index profiles.

#82452 - $15.00 USD Received 26 Apr 2007; revised 3 Jul 2007; accepted 5 Jul 2007; published 18 Jul 2007

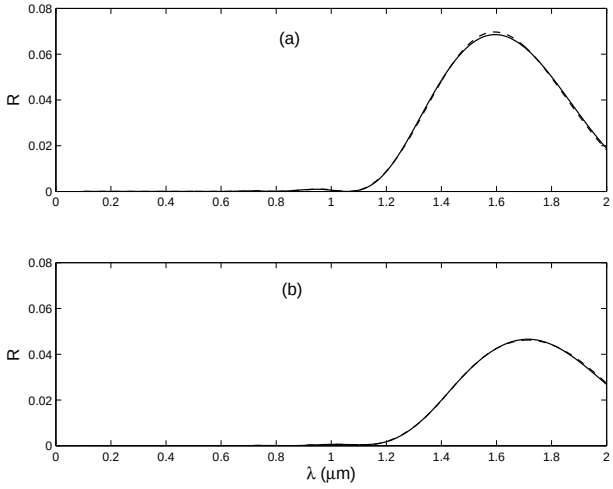

Fig. 3. Normal incidence intensity reflection coefficient R as a function of wavelength λ for the inhomogeneous film (see text for a description) (a) without or (b) with the substrate. The inhomogeneous film is designed at wavelength $1.06\mu m$. The solid (dashed) lines are for the inhomogeneous film occupying $-3\mu m \leq z \leq 3\mu m$ ($-2\mu m \leq z \leq 2\mu m$).

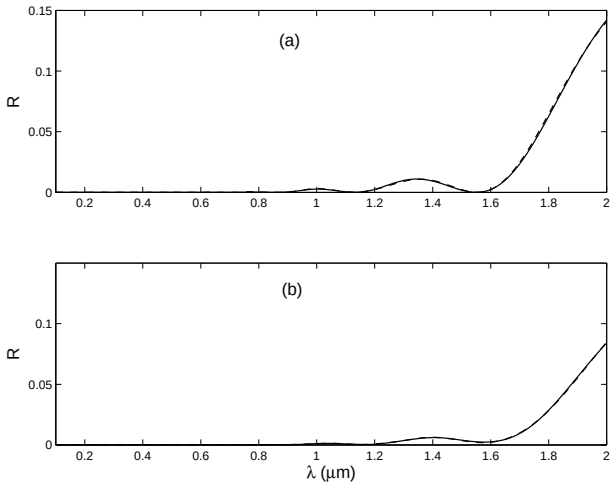

Fig. 4. Normal incidence intensity reflection coefficient R as a function of wavelength λ for the inhomogeneous film (see text for a description) (a) without or (b) with the substrate. The inhomogeneous film is designed at wavelength $1.55\mu m$. The solid (dashed) lines are for the inhomogeneous film occupying $-3\mu m \leq z \leq 3\mu m$ ($-2\mu m \leq z \leq 2\mu m$).

#82452 - $15.00 USD Received 26 Apr 2007; revised 3 Jul 2007; accepted 5 Jul 2007; published 18 Jul 2007

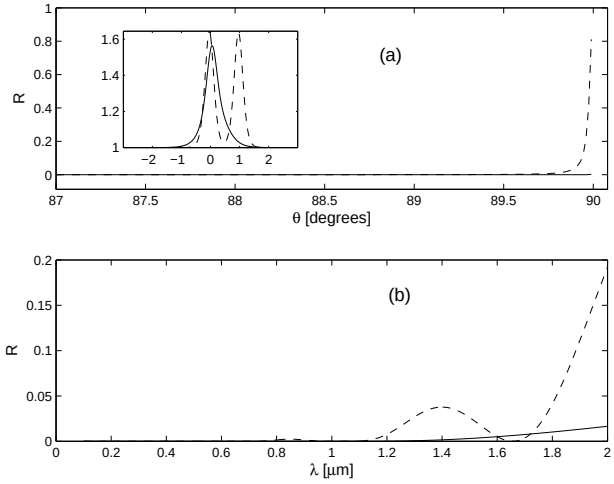

Fig. 5. Reflection coefficient R as functions of (a) angle of incidence θ for TE polarized light and (b) wavelength λ for normal incidence. The solid and dashed lines are for $A_1 = 11, A_2 = 5.5$ and $\kappa_1 = 5.5, \kappa_2 = 2.25$, i.e., for well separated eigenvalues and for $A_1 = 11, A_2 = 5.5$ and $\kappa_1 = 5.5, \kappa_2 = 5.4$, i.e., for closely spaced eigenvalues, respectively. The corresponding profiles designed at $\lambda = 1.06\mu m$ are shown in the inset.

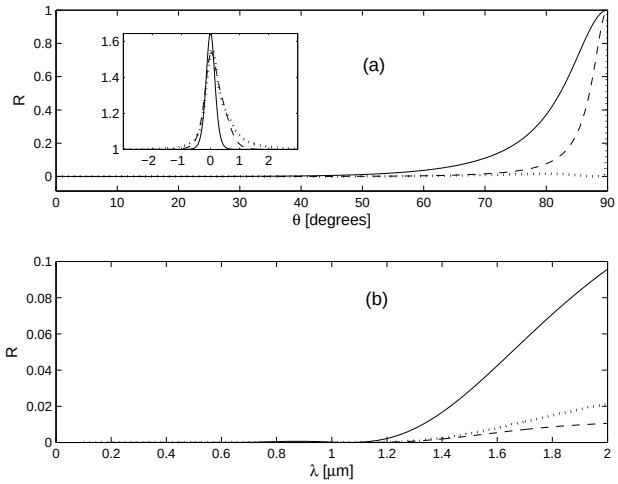

Fig. 6. Reflection coefficient R as functions of (a) angle of incidence θ for TM polarized light and (b) wavelength λ for normal incidence. The solid, dashed and dotted lines are for the parameter sets (i) $A_1 = 11$, κ_1=5.5, (ii) $A_1 = 11$, κ_1=5.5, $A_2 = 5.5$, $\kappa_2 = 2.75$, and (iii) $A_1 = 11$, κ_1=5.5, $A_2 = 5.5$, κ_2=2.75,$A_3 = 2$, κ_3=1, respectively. The corresponding profiles designed at $\lambda = 1.06\mu m$ are shown in the inset.

#82452 - $15.00 USD Received 26 Apr 2007; revised 3 Jul 2007; accepted 5 Jul 2007; published 18 Jul 2007

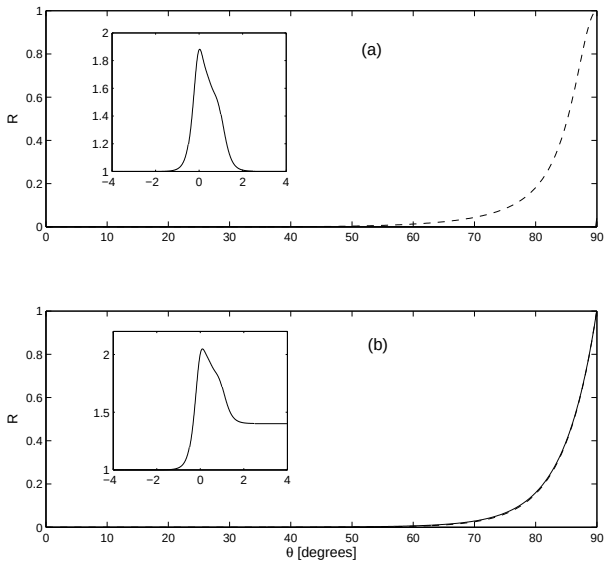

Fig. 7. Intensity reflection coefficient R as a function of angle of incidence θ for the inhomogeneous film (see text for a description) (a) without or (b) with the substrate. The inhomogeneous film (occupying $-4\mu m \leq z \leq 4\mu m$) is designed at wavelength $1.55\mu m$. The solid (dashed) lines are for TE (TM) polarization.

polarizations. Figs. 1 and 2 also demonstrate the fact that the *design principle works well for different wavelengths*.

We next investigate the wavelength dependence of the reflectivity from such films for normal incidence with or without the substrate. Results for the profiles (without and with the substrate) optimized at $\lambda = 1.06\mu m$ ($\lambda = 1.55\mu m$) are shown in Figs. 3(a) (4(a)) and 3(b) (4(b)). It is important to note that such films exhibit extremely low reflectivity over a very large range of wavelengths, though they are designed at particular wavelengths. We think that such flat response over such large spectral ranges is not achievable with conventional AR coatings based on quarter wave plates. In the same Figs. we show the *effect of truncation*. The dashed lines in Figs. 3 and 4 are for $-2\mu m \leq z \leq 2\mu m$. It is clear from the comparison that *truncation has insignificant effect* if the essential features of the inhomogeneity are retained. We carried out calculations with other higher order families of potentials in order to reveal the parameter dependence of the profiles (not shown). Larger number of parameters offer greater flexibility over the profile leading to lower reflection.

In order to highlight the effect of the eigenvalues to yield single and multiple peaked profiles, we consider two sets of parameters of the two parameter family with close-by and well separated eigenvalues. As mentioned earlier that close-by eigenvalues lead to profiles with distinct peaks. The profiles for these two cases and their effects on the reflection coefficient are shown in Fig.5. Clearly the localized profile yields better antireflection behavior.

We now demonstrate the flexibility with higher order family profiles. In order to emphasize the additional freedom, we have compared three typical cases of one, two and three parameter families in Fig.6. The results for the parameter sets (i) $A_1 = 11$, κ_1=5.5, (ii) $A_1 = 11$, κ_1=5.5, $A_2 = 5.5$, $\kappa_2 = 2.75$, and (iii) $A_1 = 11$, κ_1=5.5, $A_2 = 5.5$, κ_2=2.75,$A_3 = 2$, κ_3=1 are shown

#82452 - $15.00 USD Received 26 Apr 2007; revised 3 Jul 2007; accepted 5 Jul 2007; published 18 Jul 2007

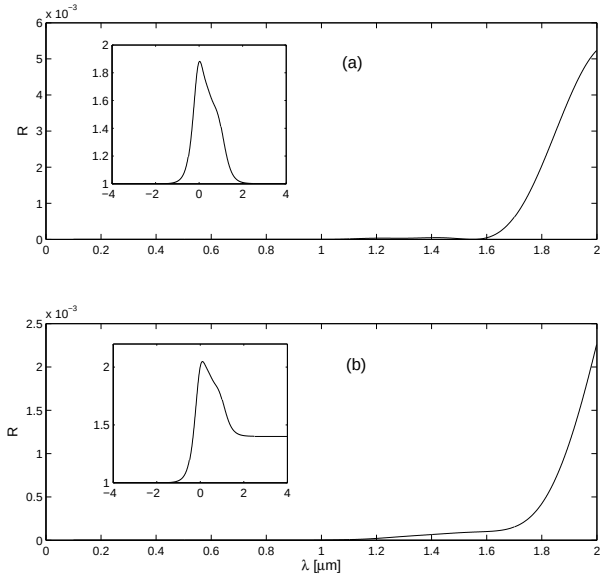

Fig. 8. Normal incidence intensity reflection coefficient R as a function of wavelength λ for the inhomogeneous film (see text for a description) (a) without or (b) with the substrate. The inhomogeneous film is designed at wavelength $1.55\mu m$. The solid (dashed) lines are for the inhomogeneous film occupying $-4\mu m \leq z \leq 4\mu m$.

by the solid, dashed and the dotted lines, respectively. It is clear from the Fig 6. that the two parameter example gives much better result than the Poschl-Teller profile in both angle and frequency scans. The three parameter profile offers better performance in the angle scan, while its frequency response slightly lags behind that of the two parameter family. However, upto the design wavelength (in this example 1.06 μm), the performances of all the three profiles are almost the same.

We next show an interesting possibility whereby a three parameter family inhomogeneous film grown on the substrate exhibits almost identical angular response for both TE and TM polarizations. The results for the profiles without and with the substrate and their response are shown in Figs. 7(b) and 8(b). The parameters were chosen as follows, $\lambda = 1.55\mu m$, $A_1 = 11.0$, $A_2 = 8.0, A_3 = 5.5$, $\kappa_1 = 5.5, \kappa_2 = 4.0, \kappa_3 = 2.25$. For comparison we have shown the results without the ramp in the upper panels of the corresponding Figs. While the angle scan for TE polarization for the profile without the ramp is significantly better than that for the TM (see Fig.7(a)), they are almost identical for the film grown on the substrate (Fig. 7(b)).

Finally it is pertinent to investigate the effect of step-size on the numerical results, since all the results were obtained based on a step-wise constant approximation of the smooth profiles. This is of practical interest since deposition of such profiles will be layer by layer with each thin layer having perhaps the same refractive index. The angle dependence of reflectivity for a PT profile occupying $-3\mu m \leq z \leq 3\mu m$ for s-polarization is shown in Fig.9 (the inset in Fig.9 shows the profile). As expected, an increasing step-size leads to a degradation of the antireflection behavior. A step-size of 0.005 μm for such profiles is accurate enough and has been used in all other calculations.

#82452 - $15.00 USD Received 26 Apr 2007; revised 3 Jul 2007; accepted 5 Jul 2007; published 18 Jul 2007

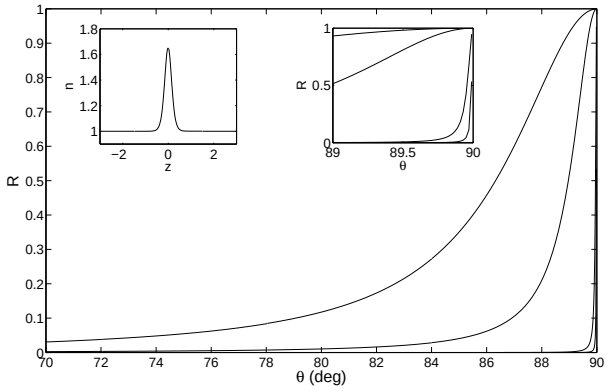

Fig. 9. Intensity reflection coefficient R as a function of angle of incidence θ for the PT profile for s-polarized light at $\lambda = 1.06\mu m$. The curves from right to left are for step-sizes 0.005, 0.01, 0.05 and 0.1 μm, respectively. The left inset shows the refractive index profile, while the right one shows the enlarged portion between 89 and 90 degrees.

4. Conclusions

In conclusion, we exploit the notion of reflectionless potentials to demonstrate a new design principle for AR coatings. We show that AR coatings designed following our method can exhibit low reflectivity over ranges of angles and wavelengths much broader than those offered by most of the existing technologies. Such refractive index profiles may be generated using the emerging technologies involving titanium oxide films [17, 18].

Acknowledgment

One of the authors (SDG) would like to thank the Council of Scientific and Industrial Research, Government of India, for partial support.

#82452 - $15.00 USD Received 26 Apr 2007; revised 3 Jul 2007; accepted 5 Jul 2007; published 18 Jul 2007